Results in Physics 19 (2020) 103330

Contents lists available at ScienceDirect

Results in Physics

journal homepage: www.elsevier.com/locate/rinp

Construction of traveling waves patterns of $(1+n)$-dimensional modified Zakharov-Kuznetsov equation in plasma physics

Adil Jhangeer[a], Maham Munawar[b], Muhammad Bilal Riaz[c,g,*], Dumitru Baleanu[d,e,f]

[a] Department of Mathematics, Namal Institute, Talagang Road, Mianwali 42250, Pakistan
[b] Department of Mathematics, University of Engineering and Technology, Pakistan
[c] Department of Mathematics, University of Management and Technology, Lahore, Pakistan
[d] Department of Mathematics, Cankaya University, Ankara, Turkey
[e] Institute of Space Sciences, Magurele, Bucharest, Romania
[f] Department of Medical Research, China Medical University, Taichung, Taiwan
[g] Institute for Groundwater Studies, University of the Free State, South Africa

ARTICLE INFO

Keywords:
Modified Zakharov-Kuznetsov equation
Soliton solutions
Cubic Duffing equation
The extended $(\frac{G'}{G^2})$-expansion method
New extended algebraic method

ABSTRACT

In this research, we examine the modified model of $(1+n)$-dimensional Zakharov-Kuznetsov (ZK) equation, which will be used to analyze the nature of weakly nonlinear traveling waves in the existence of a constant magnetic area in a plasma comprising in cold ions and hot isothermal electrons. The modified Zakharov-Kuznetsov (mZK) equation will have solutions describing the traveling solitary waves, using the extended $(\frac{G'}{G^2})$-expansion method and extended direct algebraic method gives way to the mZK equation regulating the transmission of ion dynamics for nonlinear traveling waves in a plasma. The sufficient conditions for the stability and existence of the traveling wave solutions are reported. Semi-dark, rational, and singular solitary wave solutions are computed. Graphical interpretations of certain practical solutions for specific values of parameters have also been available. The research findings reported throughout this evaluation are fresh and from which this model is employed to analyze waves in numerous plasmas, could be valuable and important. Subsequently, there are concluding remarks mentioned.

Introduction

Nonlinear physical structures have been linked with nonlinear equations concerning several disciplines, like thermodynamics, mechanics, fluid dynamics, wave propagation, plasma physics, fluid flow, nonlinear networks, optical fibers, and soil consolidations to develop vital phenomenon and implementations. The role of non-linearity in waves is quite significant mostly throughout nonlinear sciences, research development towards exact solutions of partial differential nonlinear equations has always been a major endeavor for the past couple of years. Hence, highly prominent areas of general interest are still the discovery of the exact analytical solutions for differential nonlinear equations. Most other investigations have thus far concentrated on developing new modifications of current methods to produce new exact analytical approaches from which it can define perhaps some difficult and complicated physical implementations. Within the past couple of years, with either the advancement of symbolic computational programs which assist us enough to conduct tedious and complex calculation on computer systems, most research has appeared to be based on direct methods to establishing exact analytical solutions for differential nonlinear equations. All the while, several powerful, efficient, and reliable methods for attempting to seek exact analytical solutions to traveling waves have been established. As for illustration, Exp-function [1], F-expansion [2], the Backlund transformation method [3,4], reductive perturbation [5], the tanh-function [6,7], Jacobi elliptic [8,9], sine cosine function methods [10], homogeneous balance method [11,12] as well as the novel $(\frac{G'}{G})$ -expansion method [13]. Nonlinear partial differential equations perform a particularly significant key position in explaining the complex algorithms that occur in various fields of science. Resolving these nonlinear structures is thus a fruitful sector of study for researchers since the solutions that arise will support and help describe the physical nature of the underlying problems particularly concerned.

Plasma physics is the investigation of a form of matter that includes charged particles. Commonly plasmas are generated by heating a gas till the electrons are dissociated from their parent molecule, briefly, a

* Corresponding author.
E-mail address: bilal.riaz@umt.edu.pk (M.B. Riaz).

https://doi.org/10.1016/j.rinp.2020.103330
Received 18 July 2020; Received in revised form 11 August 2020; Accepted 12 August 2020
Available online 28 August 2020

plasma is known as an ionized gas. Plasma physics does seem to be the analysis of charged particles as well as fluids that interact with self-consistent magnetic and electrical fields. It would be a fundamental discipline of research that has several distinct application areas, such as astrophysics and space, accelerator physics, controlled fusion also beam storage. In magnetized plasma, the ZK equation has been structured for analyzing the nonlinear propagation of ion-acoustic waves. The ZK equation to analyzing vortices for geophysical flows is a really interesting prototype equation. It makes an appearance especially throughout the research area of plasma physics. The ZK equation that based totally on the expression of nonlinear weakly ion-acoustic waves in plasma that comprises hot isothermal electrons and cold ions, when the occupied field is uniformly magnetic [14]. This may be recognized here as the following form [15]:

$$u_t + \beta u u_x + (\nabla^2 u)_x = 0, \tag{1}$$

in which $\nabla^2 = \partial_x^2 + \partial_y^2 + \partial_z^2$, is Laplacian, while β is a constant.

Various techniques have been employed in literary history to figure out the exact analytical solutions as well as conservation laws of the ZK equation [16–20]. Unless the plasma becomes magnetized then the leading equation is ZK equation while the electrons are iso-thermal. Stability of the ZK equation's plane-periodic and solitary wave solutions to 2D long-wavelength perturbations [21,22], have already been analyzed.

Here, we took into consideration $(1 + n)$-dimensional mZK equation of the form:

$$u_t + \beta u^2 u_{x_1} + (\nabla^2 u)_{x_1} = 0, \tag{2}$$

where $\nabla^2 = \partial_{x_1}^2 + \partial_{x_2}^2 + \partial_{x_3}^2 + \ldots + \partial_{x_\Gamma}^2$, is the n-dimensional Laplacian also the wave profile is designated by the dependent variable u which depends on the independent variables i.e, temporal variable t and structural variable x respectively, while β is a real constant. To analyze the waves in plasma physics, the exact solutions of the $(1 + n)$-dimensional mZK equation [15,23–29].

The solitary electromagnetic frameworks noticed to occur in a certain debased EP plasma are considerably modified by the consequences of both pressure dependence of positron as well as the degenerate electron. The observations refer to an EP plasma medium that exists in astrophysical compact entities [30,31]. The analysis of traveling waves has been given in [32], for the ZK equation. Employing improved modified extended tanh-function method soliton solutions are obtained [33]. Periodic solutions, one-dimensional soliton, apparently inelastic, and N-soliton solutions have been achieved. The direct Hirota bilinear method and the auxiliary equation method were used for the quantum ZK equation in [34–37]. Significantly over the past couple of years, in either the context of computational mathematics, other methods of searching exact outcomes of differential nonlinear equations motivated by the $(\frac{G'}{G})$-expansion method. By instance, the $(\frac{1}{G'})$-expansion [38], double $((\frac{G'}{G}), (\frac{1}{G}))$ [39,40], the extended $(\frac{G'}{G})$-expansion, modified $(\frac{G'}{G})$-expansion methods [41–46] and the extended $(\frac{G'}{G^2})$-expansion method [47–50]. The whole article intends to extract more new exact solitary wave solutions of the mZK equation. To obtain these solitary wave solutions we will employ the extended $(\frac{G'}{G^2})$-expansion method [47–49] and the extended direct algebraic method [51–53] to solve $(1 + n)$-dimensional mZK equation. Some completely new, exact solitary wave solutions are derived from $(1 + n)$-dimensional mZK equation.

Recently, soliton theory has increasingly been recognized as one of the widely studied fields of science. Several analogous work is quoted regarding analytic solutions, such as [54–62]. Multiple physical structures may be smoothly and efficiently modeled through equations that admit soliton solutions. Evidently, in several other scenarios soliton itself and solitary waves were observed yet often dominate long-term behavior. Soliton-solution equations have quite an extremely deep mathematical structure [59,63–74]. The background and mathematical structures of solitons of the Shrödinger nonlinear equation and KdV equation (Korteweg and de Vries) nowadays are analyzed in greater depth [55,62,72,75,73,76]. Solitons perform a crucial function in numerous fields and because of their production and regulation of optical fibers are greatly essential of optics. Soliton dynamics in the manner of optical fibers is one of the impressive work areas mostly in telecommunications, electrical engineering, and applied sciences. Due to its impressive advancement in the field of optical fibers, the telecommunications system has witnessed significant growth, especially in recent decades [77–80]. Exploring the traveling wave solutions for linear and nonlinear equations has played a vital part not only in mathematics but also for engineering and other nonlinear research in the last few decades [59,68,69,75,76,81–84].

This paper is set out as follows. In Section "The portrayal of two integration techniques", there is dedicated to showing the portrayal of methodology for the extended $(\frac{G'}{G^2})$-expansion method and the extended direct algebraic method. In Section "Application to mZK equation", there is a transformation of the mZK equation into the famous cubic Duffing equation. In Section "The extended $(\frac{G'}{G^2})$-expansion method", there is the implementation of the extended $(\frac{G'}{G^2})$-expansion method to the transformed mZK equation with sufficient conditions for stability of traveling wave solutions along with the graphical representations. In Section "The extended direct algebraic method", the implementation of the extended direct algebraic method to the transformed mZK equation along with the graphical representations of the results. In Section "Concluding remarks", the paper ultimately finishes with concluding remarks.

The portrayal of two integration techniques

The extended $(\frac{G'}{G^2})$-expansion method

Consider a nonlinear partial differential equation with u as the dependent variable and $(t, x_1, x_2, \ldots, x_\Gamma)$ as independent variables of the form:

$$Q(u, u_t, u_{x_1}, u_{x_2}, \ldots) = 0, \tag{3}$$

using the transformation $u(t, x_1, x_2, \ldots, x_\Gamma) = U(\xi)$, $\xi = x_1 + x_2 + x_3 + \ldots + x_\Gamma - \alpha t$ where α is the speed of wave traveled. It will convert Eq. (3) into nonlinear ordinary differential equation of the following form

$$Q(U, U', U'', \ldots) = 0, \tag{4}$$

where prime denotes the derivative with respect to ξ. Suppose Eq. (4) has the solution of form:

$$U(\xi) = a_{M+1} + \sum_{i=1}^{M}\left[a_i\left(\frac{G'}{G^2}\right) + a^i\left(\frac{G'}{G^2}\right)^{-1}\right], \tag{5}$$

where

$$\left(\frac{G'}{G^2}\right)' = \mu + \lambda\left(\frac{G'}{G^2}\right)^2, \tag{6}$$

where μ and λ are the real constants.

General solutions for Eq. (6) with respect to parameters μ along with λ are given as follows.

(1): If $\mu\lambda > 0$

$$\left(\frac{G'}{G^2}\right)' = \sqrt{\frac{\mu}{\lambda}}\left[\frac{r_1\cos(\sqrt{\mu\lambda}\,\xi) + r_2\sin(\sqrt{\mu\lambda}\,\xi)}{r_2\cos(\sqrt{\mu\lambda}\,\xi) - r_1\sin(\sqrt{\mu\lambda}\,\xi)}\right]. \tag{7}$$

(2): If $\mu\lambda < 0$

$$\left(\frac{G'}{G^2}\right)' = -\frac{\sqrt{|\mu\lambda|}}{\lambda}\left[\frac{r_1\sinh(2\sqrt{|\mu\lambda|}\,\xi) + r_1\cosh(2\sqrt{|\mu\lambda|}\,\xi) + r_2}{r_1\sinh(2\sqrt{|\mu\lambda|}\,\xi) + r_1\cosh(2\sqrt{|\mu\lambda|}\,\xi) - r_2}\right]. \tag{8}$$

(3): If $\mu = 0, \lambda \neq 0$

$$\left(\frac{G'}{G^2}\right)' = -\left[\frac{r_1}{\lambda(r_1\xi + r_2)}\right]. \tag{9}$$

After plugging Eq. (5) in Eq. (4) and equating the coefficients of different powers of $(\frac{G'}{G^2})$ leads to a set of algebraic equations (with some more detailed information check [47–50]). With the aid of computational program, the system of algebraic equations can be solved and solutions of Eq. (4) with the help of (7)-(9) can be derived.

The extended direct algebraic method

Let us considered Eq. (4) has the solution of the pattern:

$$U(\xi) = a_0 + \sum_{i=1}^{M}[a_i W(\xi)], \tag{10}$$

where

$$W'(\xi) = ln(\rho)(\mu + \nu W(\xi) + \zeta W^2(\xi)),\ \ \rho \neq 0, 1. \tag{11}$$

Here ν, μ along with ζ are the real constants and M that is a constant which can be evaluated by balancing the highest order derivative along with nonlinear terms of Eq. (4).

General solutions of Eq. (11) as regards with parameters ν, μ and ζ are follows (with some more detailed information check [51,52]): where $\Phi = \nu^2 - 4\mu\zeta$.

(1): If $\Phi < 0$ and $\zeta \neq 0$,

$$W_1(\xi) = -\frac{\nu}{2\zeta} + \frac{\sqrt{-\Phi}}{2\zeta}\tan_\rho\left(\frac{\sqrt{-\Phi}}{2}\xi\right), \tag{12}$$

$$W_2(\xi) = -\frac{\nu}{2\zeta} - \frac{\sqrt{-\Phi}}{2\zeta}\cot_\rho\left(\frac{\sqrt{-\Phi}}{2}\xi\right), \tag{13}$$

$$W_3(\xi) = -\frac{\nu}{2\zeta} + \frac{\sqrt{-\Phi}}{2\zeta}(\tan_\rho(\sqrt{-(\Phi)}\xi) \pm \sqrt{mn}\sec_\rho(\sqrt{-(\Phi)}\xi)), \tag{14}$$

$$W_4(\xi) = -\frac{\nu}{2\zeta} + \frac{\sqrt{-\Phi}}{2\zeta}(\cot_\rho(\sqrt{-\Phi}\xi) \pm \sqrt{mn}\csc_\rho(\sqrt{-\Phi}\xi)), \tag{15}$$

$$W_5(\xi) = -\frac{\nu}{2\zeta} + \frac{\sqrt{-\Phi}}{4\zeta}\left(\tan_\rho\left(\frac{\sqrt{-\Phi}}{4}\xi\right) - \cot_\rho\left(\frac{\sqrt{-\Phi}}{4}\xi\right)\right). \tag{16}$$

(2): If $\Phi > 0$ and $\zeta \neq 0$,

$$W_6(\xi) = -\frac{\nu}{2\zeta} - \frac{\sqrt{\Phi}}{2\zeta}\tanh_\rho\left(\frac{\sqrt{\Phi}}{2}\xi\right), \tag{17}$$

$$W_7(\xi) = -\frac{\nu}{2\zeta} - \frac{\sqrt{\Phi}}{2\zeta}\coth_\rho\left(\frac{\sqrt{\Phi}}{2}\xi\right), \tag{18}$$

$$W_8(\xi) = -\frac{\nu}{2\zeta} + \frac{\sqrt{\Phi}}{2\zeta}(-\tanh_\rho(\sqrt{\Phi}\xi) \pm i\sqrt{mn}\,\mathrm{sech}_\rho(\sqrt{\Phi}\xi)), \tag{19}$$

$$W_9(\xi) = -\frac{\nu}{2\zeta} + \frac{\sqrt{\Phi}}{2\zeta}(-\coth_\rho(\sqrt{\Phi}\xi) \pm \sqrt{mn}\,\mathrm{csch}_\rho(\sqrt{\Phi}\xi)), \tag{20}$$

$$W_{10}(\xi) = -\frac{\nu}{2\zeta} - \frac{\sqrt{\Phi}}{4\zeta}\left(\tanh_\rho\left(\frac{\sqrt{\Phi}}{4}\xi\right) + \coth_\rho\left(\frac{\sqrt{\Phi}}{4}\xi\right)\right). \tag{21}$$

(3): If $\mu\zeta > 0$ and $\nu = 0$,

$$W_{11}(\xi) = \sqrt{\frac{\mu}{\zeta}}\tan_\rho(\sqrt{\mu\zeta}\xi), \tag{22}$$

$$W_{12}(\xi) = -\sqrt{\frac{\mu}{\zeta}}\cot_\rho(\sqrt{\mu\zeta}\xi), \tag{23}$$

$$W_{13}(\xi) = \sqrt{\frac{\mu}{\zeta}}(\tan_\rho(2\sqrt{\mu\zeta}\xi) \pm \sqrt{mn}\sec_\rho(2\sqrt{\mu\zeta}\xi)), \tag{24}$$

$$W_{14}(\xi) = \sqrt{\frac{\mu}{\zeta}}(-\cot_\rho(2\sqrt{\mu\zeta}\xi) \pm \sqrt{mn}\csc_\rho(2\sqrt{\mu\zeta}\xi)), \tag{25}$$

$$W_{15}(\xi) = \frac{1}{2}\sqrt{\frac{\mu}{\zeta}}\left(\tan_\rho\left(\frac{\sqrt{\mu\zeta}}{2}\xi\right) - \cot_\rho\left(\frac{\sqrt{\mu\zeta}}{2}\xi\right)\right). \tag{26}$$

(4): If $\mu\zeta < 0$ and $\nu = 0$,

$$W_{16}(\xi) = -\sqrt{-\frac{\mu}{\zeta}}\tanh_\rho(\sqrt{-\mu\zeta}\xi), \tag{27}$$

$$W_{17}(\xi) = -\sqrt{-\frac{\mu}{\zeta}}\coth_\rho(\sqrt{-\mu\zeta}\xi), \tag{28}$$

$$W_{18}(\xi) = \sqrt{-\frac{\mu}{\zeta}}(-\tanh_\rho(2\sqrt{-\mu\zeta}\xi) \pm i\sqrt{mn}\,\mathrm{sech}_\rho(2\sqrt{-\mu\zeta}\xi)), \tag{29}$$

$$W_{19}(\xi) = \sqrt{-\frac{\mu}{\zeta}}(-\coth_\rho(2\sqrt{-\mu\zeta}\xi) \pm \sqrt{mn}\,\mathrm{csch}_\rho(2\sqrt{-\mu\zeta}\xi)), \tag{30}$$

$$W_{20}(\xi) = -\frac{1}{2}\sqrt{-\frac{\mu}{\zeta}}\left(\tanh_\rho\left(\frac{\sqrt{-\mu\zeta}}{2}\xi\right) + \coth_\rho\left(\frac{\sqrt{-\mu\zeta}}{2}\xi\right)\right). \tag{31}$$

(5): If $\nu = 0$ and $\mu = \zeta$,

$$W_{21}(\xi) = \tan_\rho(\mu\xi), \tag{32}$$

$$W_{22}(\xi) = -\cot_\rho(\mu\xi), \tag{33}$$

$$W_{23}(\xi) = \tan_\rho(2\mu\xi) \pm \sqrt{mn}\sec_\rho(2\mu\xi), \tag{34}$$

$$W_{24}(\xi) = -\cot_\rho(2\mu\xi) \pm \sqrt{mn}\csc_\rho(2\mu\xi), \tag{35}$$

$$W_{25}(\xi) = \frac{1}{2}\left(\tan_\rho\left(\frac{\mu}{2}\xi\right) - \cot_\rho\left(\frac{\mu}{2}\xi\right)\right). \quad (36)$$

(6): If $\nu = 0$ and $\zeta = -\mu$,

$$W_{26}(\xi) = -\tanh_\rho(\mu\xi), \quad (37)$$

$$W_{27}(\xi) = -\coth_\rho(\mu\xi), \quad (38)$$

$$W_{28}(\xi) = -\tanh_\rho(2\mu\xi) \pm i\sqrt{mn}\,\mathrm{sech}_\rho(2\mu\xi), \quad (39)$$

$$W_{29}(\xi) = -\cot_\rho(2\mu\xi) \pm \sqrt{mn}\,\mathrm{csch}_\rho(2\mu\xi), \quad (40)$$

$$W_{30}(\xi) = -\frac{1}{2}\tanh_\rho\left(\frac{\mu}{2}\xi\right) + \cot_\rho\left(\frac{\mu}{2}\xi\right). \quad (41)$$

(7): If $\nu^2 = 4\mu\zeta$,

$$W_{31}(\xi) = \frac{-2\mu(\nu\xi\ln\rho + 2)}{\nu^2\xi\ln\rho}. \quad (42)$$

(8): If $\nu = p$, $\mu = pq$, $(q \neq 0)$ and $\zeta = 0$,

$$W_{32}(\xi) = \rho^{p\xi} - q. \quad (43)$$

(9): If $\nu = \zeta = 0$,

$$W_{33}(\xi) = \mu\xi\ln\rho. \quad (44)$$

(10): If $\nu = \mu = 0$,

$$W_{34}(\xi) = \frac{-1}{\zeta\xi\ln\rho}. \quad (45)$$

(11): If $\mu = 0$ and $\nu \neq 0$,

$$W_{35}(\xi) = -\frac{m\nu}{\zeta(\cosh_\rho(\nu\xi) - \sinh_\rho(\nu\xi) + m)}, \quad (46)$$

$$W_{36}(\xi) = -\frac{\nu(\sinh_\rho(\nu\xi) + \cosh_\rho(\nu\xi))}{\zeta(\sinh_\rho(\nu\xi) + \cosh_\rho(\nu\xi) + n)}. \quad (47)$$

(12): If $\nu = p$, $\zeta = pq$, $(q \neq 0$ and $\mu = 0)$,

$$W_{37}(\xi) = -\frac{m\rho^{p\xi}}{m - qn\rho^{p\xi}}. \quad (48)$$

$$\sinh_\rho(\xi) = \frac{m\rho^\xi - n\rho^{-\xi}}{2},\ \cosh_\rho(\xi) = \frac{m\rho^\xi + n\rho^{-\xi}}{2},$$

$$\tanh_\rho(\xi) = \frac{m\rho^\xi - n\rho^{-\xi}}{m\rho^\xi + n\rho^{-\xi}},\ \coth_\rho(\xi) = \frac{m\rho^\xi + n\rho^{-\xi}}{m\rho^\xi - n\rho^{-\xi}},$$

$$\mathrm{sech}_\rho(\xi) = \frac{2}{m\rho^\xi + n\rho^{-\xi}},\ \mathrm{csch}_\rho(\xi) = \frac{2}{m\rho^\xi - n\rho^{-\xi}},$$

$$\sin_\rho(\xi) = \frac{m\rho^{i\xi} - n\rho^{-i\xi}}{2i},\ \cos_\rho(\xi) = \frac{m\rho^{i\xi} + n\rho^{-i\xi}}{2},$$

$$\tan_\rho(\xi) = -i\frac{m\rho^{i\xi} - n\rho^{-i\xi}}{m\rho^{i\xi} + n\rho^{-i\xi}},\ \cot_\rho(\xi) = i\frac{m\rho^{i\xi} + n\rho^{-i\xi}}{m\rho^{i\xi} - n\rho^{-i\xi}},$$

$$\sec_\rho(\xi) = \frac{2}{m\rho^\xi + n\rho^{-\xi}},\ \csc_\rho(\xi) = \frac{2i}{m\rho^\xi - n\rho^{-\xi}},$$

where m and n are called parameters of deformation.

Application to mZK equation

In this whole portion, we are going to apply the following wave transformation on Eq. (2) to transform the original PDE into an ODE, so that traveling wave solutions can be determined:

$$\xi = x_1 + x_2 + x_3 + \ldots + x_\Gamma - \alpha t, \quad (49)$$

where α is the speed of wave traveled, it will transform Eq. (2) into an ODE as given below

$$-\alpha U_\xi + \beta U^2 U_\xi + \Gamma U_{\xi\xi\xi} = 0, \quad (50)$$

where $U = U(\xi) = u(t, X) = u(t, x_1, x_2, x_3, \ldots, x_\Gamma)$ and $U_\xi = \frac{du}{d\xi}$.

Integrating once, by taking constant of integration as zero. The above equation becomes

$$-\alpha U + \frac{\beta}{3}U^3 + \Gamma U_{\xi\xi} = 0, \quad (51)$$

where α, β and Γ are real-valued parameters.

The extended $(\frac{G'}{G^2})$-expansion method

The next aim is to obtain a solution of Eq. (51). For traveling wave solutions of Eq. (2), one needs to solve only Eq. (51). Suppose the solution of Eq. (51) can be represented here as finite power series of the format:

$$U(\xi) = a_2 + a_1\left(\frac{G'}{G^2}\right) + a_{-1}\left(\frac{G'}{G^2}\right)^{-1}, \quad (52)$$

where a_2, a_1 and a_{-1} are constants. After substituting Eq. (52) in Eq. (51) using Eq. (6) and equating coefficients of different powers of $(\frac{G'}{G^2})$, leads to a system of following algebraic equations.

$$\left(\frac{G'}{G^2}\right)^{-3}: 2\Gamma\mu^2 a_{-1} + \frac{1}{3}\beta a_{-1}^3 = 0,$$

$$\left(\frac{G'}{G^2}\right)^{-2}: \beta a_{-1}^2 a_2 = 0,$$

$$\left(\frac{G'}{G^2}\right)^{-1}: -\alpha a_{-1} + 2\Gamma\lambda\mu a_{-1} + \beta a_{-1}^2 a_1 + \beta a_{-1} a_2^2 = 0,$$

$$\left(\frac{G'}{G^2}\right)^{0}: -\alpha a_2 + 2\beta a_{-1} a_1 a_2 + \frac{1}{3}\beta a_2^3 = 0,$$

$$\left(\frac{G'}{G^2}\right)^{1}: -\alpha a_1 + 2\Gamma\lambda\mu a_1 + \beta a_{-1} a_1^2 + \beta a_1 a_2^2 = 0,$$

$$\left(\frac{G'}{G^2}\right)^{2}: \beta a_1^2 a_2 = 0,$$

$$\left(\frac{G'}{G^2}\right)^3: 2\Gamma\lambda^2 a_1 + \frac{1}{3}\beta a_1^3 = 0.$$

Resolving the above algebraic equations with the aid of computational program, following different nontrivial solutions are achieved.

Set 1:

$$a_{-1} = \pm\sqrt{\frac{3\alpha\mu}{2\beta\lambda}},\quad a_1 = \pm\sqrt{\frac{3\alpha\lambda}{2\beta\mu}},\quad a_2 = 0,\quad \Gamma = -\frac{\alpha}{4\lambda\mu}. \tag{53}$$

Set 2:

$$a_{-1} = \pm\frac{1}{2}\sqrt{\frac{-3\alpha\mu}{\beta\lambda}},\quad a_1 = \mp\frac{1}{2}\sqrt{\frac{-3\alpha\lambda}{\beta\mu}},\quad a_2 = 0,\quad \Gamma = -\frac{\alpha}{8\lambda\mu}. \tag{54}$$

When we substitute these respective sets of values in Eq. (52) it will give the exact solutions of $(1+n)$-dimensional mZK equation.

Set 1

$\mu\lambda > 0$

The solution is given in (53), utilizing Eq. (52) refers to a solution below:

$$U_1(\xi) = \pm\sqrt{\frac{3\alpha}{2\beta}}\left[\frac{c_1\cos(\sqrt{\mu\lambda}\,\xi) + c_2\sin(\sqrt{\mu\lambda}\,\xi)}{c_2\cos(\sqrt{\mu\lambda}\,\xi) - c_1\sin(\sqrt{\mu\lambda}\,\xi)}\right] \pm \sqrt{\frac{3\alpha}{2\beta}}\left[\frac{c_2\cos(\sqrt{\mu\lambda}\,\xi) - c_1\sin(\sqrt{\mu\lambda}\,\xi)}{c_1\cos(\sqrt{\mu\lambda}\,\xi) + c_2\sin(\sqrt{\mu\lambda}\,\xi)}\right],$$

$U_1(\xi)$ with Eq. (49) generates the following solution of Eq. (2),

$$u_1(t,X) = \pm\sqrt{\frac{3\alpha}{2\beta}}\left[\frac{c_1\cos(\sqrt{\mu\lambda}(x_1+x_2+\ldots+x_\Gamma-\alpha t)) + c_2\sin(\sqrt{\mu\lambda}(x_1+x_2+\ldots+x_\Gamma-\alpha t))}{c_2\cos(\sqrt{\mu\lambda}(x_1+x_2+\ldots+x_\Gamma-\alpha t)) - c_1\sin(\sqrt{\mu\lambda}(x_1+x_2+\ldots+x_\Gamma-\alpha t))}\right] \pm \sqrt{\frac{3\alpha}{2\beta}}\left[\frac{c_2\cos(\sqrt{\mu\lambda}(x_1+x_2+\ldots+x_\Gamma-\alpha t)) - c_1\sin(\sqrt{\mu\lambda}(x_1+x_2+\ldots+x_\Gamma-\alpha t))}{c_1\cos(\sqrt{\mu\lambda}(x_1+x_2+\ldots+x_\Gamma-\alpha t)) + c_2\sin(\sqrt{\mu\lambda}(x_1+x_2+\ldots+x_\Gamma-\alpha t))}\right].$$

$\mu\lambda < 0$

Here, for this case solution in (53) with the aid of Eq. (52) gives, which yields:

$$U_2(\xi) = \mp\sqrt{\frac{3\alpha}{2\beta}}\left[\sqrt{\frac{|\mu\lambda|}{\mu\lambda}}\left(\frac{c_1\sinh(2\sqrt{|\mu\lambda|}\,\xi) + c_1\cosh(2\sqrt{|\mu\lambda|}\,\xi) + c_2}{c_1\sinh(2\sqrt{|\mu\lambda|}\,\xi) + c_1\cosh(2\sqrt{|\mu\lambda|}\,\xi) - c_2}\right)\right] \mp \sqrt{\frac{3\alpha}{2\beta}}\left[\sqrt{\frac{\mu\lambda}{|\mu\lambda|}}\left(\frac{c_1\sinh(2\sqrt{|\mu\lambda|}\,\xi) + c_1\cosh(2\sqrt{|\mu\lambda|}\,\xi) - c_2}{c_1\sinh(2\sqrt{|\mu\lambda|}\,\xi) + c_1\cosh(2\sqrt{|\mu\lambda|}\,\xi) + c_2}\right)\right],$$

$U_2(\xi)$ with Eq. (49) generates the following solution of Eq. (2),

$$u_2(t,X) = \mp\sqrt{\frac{3\alpha}{2\beta}}\left[\sqrt{\frac{|\mu\lambda|}{\mu\lambda}}\left(\frac{c_1\sinh(2\sqrt{|\mu\lambda|}(x_1+x_2+\ldots+x_\Gamma-\alpha t)) + c_1\cosh(2\sqrt{|\mu\lambda|}(x_1+x_2+\ldots+x_\Gamma-\alpha t)) + c_2}{c_1\sinh(2\sqrt{|\mu\lambda|}(x_1+x_2+\ldots+x_\Gamma-\alpha t)) + c_1\cosh(2\sqrt{|\mu\lambda|}(x_1+x_2+\ldots+x_\Gamma-\alpha t)) - c_2}\right)\right] \mp \sqrt{\frac{3\alpha}{2\beta}}\left[\sqrt{\frac{\mu\lambda}{|\mu\lambda|}}\left(\frac{c_1\sinh(2\sqrt{|\mu\lambda|}(x_1+x_2+\ldots+x_\Gamma-\alpha t)) + c_1\cosh(2\sqrt{|\mu\lambda|}(x_1+x_2+\ldots+x_\Gamma-\alpha t)) - c_2}{c_1\sinh(2\sqrt{|\mu\lambda|}(x_1+x_2+\ldots+x_\Gamma-\alpha t)) + c_1\cosh(2\sqrt{|\mu\lambda|}(x_1+x_2+\ldots+x_\Gamma-\alpha t)) + c_2}\right)\right].$$

Set 2

$\mu\lambda > 0$

Act along the same lines as in the previous set, solution demonstrated in (54), via Eq. (52) refers to corresponding solution:

$$U_3(\xi) = \pm\frac{1}{2}\sqrt{\frac{-3\alpha}{\beta}}\left[\frac{c_1\cos(\sqrt{\mu\lambda}\,\xi) + c_2\sin(\sqrt{\mu\lambda}\,\xi)}{c_2\cos(\sqrt{\mu\lambda}\,\xi) - c_1\sin(\sqrt{\mu\lambda}\,\xi)}\right] \pm \frac{1}{2}\sqrt{\frac{-3\alpha}{\beta}}\left[\frac{c_2\cos(\sqrt{\mu\lambda}\,\xi) - c_1\sin(\sqrt{\mu\lambda}\,\xi)}{c_1\cos(\sqrt{\mu\lambda}\,\xi) + c_2\sin(\sqrt{\mu\lambda}\,\xi)}\right],$$

$U_3(\xi)$ with Eq. (49) generates the following solution of Eq. (2),

$$u_3(t,X) = \pm\frac{1}{2}\sqrt{\frac{-3\alpha}{\beta}}\left[\frac{c_1\cos(\sqrt{\mu\lambda}(x_1+x_2+\ldots+x_\Gamma-\alpha t)) + c_2\sin(\sqrt{\mu\lambda}(x_1+x_2+\ldots+x_\Gamma-\alpha t))}{c_2\cos(\sqrt{\mu\lambda}(x_1+x_2+\ldots+x_\Gamma-\alpha t)) - c_1\sin(\sqrt{\mu\lambda}(x_1+x_2+\ldots+x_\Gamma-\alpha t))}\right] \pm \frac{1}{2}\sqrt{\frac{-3\alpha}{\beta}}\left[\frac{c_2\cos(\sqrt{\mu\lambda}(x_1+x_2+\ldots+x_\Gamma-\alpha t)) - c_1\sin(\sqrt{\mu\lambda}(x_1+x_2+\ldots+x_\Gamma-\alpha t))}{c_1\cos(\sqrt{\mu\lambda}(x_1+x_2+\ldots+x_\Gamma-\alpha t)) + c_2\sin(\sqrt{\mu\lambda}(x_1+x_2+\ldots+x_\Gamma-\alpha t))}\right].$$

$\mu\lambda < 0$

Here, solution behind this case in (54) with the assistance of Eq. (52) contribute, which produces:

$$U_4(\xi) = \pm\frac{1}{2}\sqrt{\frac{-3\alpha}{\beta}}\sqrt{\frac{|\mu\lambda|}{\mu\lambda}}\left[\frac{c_1\sinh(2\sqrt{|\mu\lambda|}\,\xi) + c_1\cosh(2\sqrt{|\mu\lambda|}\,\xi) + c_2}{c_1\sinh(2\sqrt{|\mu\lambda|}\,\xi) + c_1\cosh(2\sqrt{|\mu\lambda|}\,\xi) - c_2}\right] \mp \frac{1}{2}\sqrt{\frac{-3\alpha}{\beta}}\sqrt{\frac{\mu\lambda}{|\mu\lambda|}}\left[\frac{c_1\sinh(2\sqrt{|\mu\lambda|}\,\xi) + c_1\cosh(2\sqrt{|\mu\lambda|}\,\xi) - c_2}{c_1\sinh(2\sqrt{|\mu\lambda|}\,\xi) + c_1\cosh(2\sqrt{|\mu\lambda|}\,\xi) + c_2}\right],$$

$U_4(\xi)$ with Eq. (49) generates the following solution of Eq. (2),

$$u_4(t,X) = \pm\frac{1}{2}\sqrt{\frac{-3\alpha}{\beta}}\sqrt{\frac{|\mu\lambda|}{\mu\lambda}}\left[\frac{c_1\sinh(2\sqrt{|\mu\lambda|}(x_1+x_2+\ldots+x_\Gamma-\alpha t)) + c_1\cosh(2\sqrt{|\mu\lambda|}(x_1+x_2+\ldots+x_\Gamma-\alpha t)) + c_2}{c_1\sinh(2\sqrt{|\mu\lambda|}(x_1+x_2+\ldots+x_\Gamma-\alpha t)) + c_1\cosh(2\sqrt{|\mu\lambda|}(x_1+x_2+\ldots+x_\Gamma-\alpha t)) - c_2}\right] \mp \frac{1}{2}\sqrt{\frac{-3\alpha}{\beta}}\sqrt{\frac{\mu\lambda}{|\mu\lambda|}}\left[\frac{c_1\sinh(2\sqrt{|\mu\lambda|}(x_1+x_2+\ldots+x_\Gamma-\alpha t)) + c_1\cosh(2\sqrt{|\mu\lambda|}(x_1+x_2+\ldots+x_\Gamma-\alpha t)) - c_2}{c_1\sinh(2\sqrt{|\mu\lambda|}(x_1+x_2+\ldots+x_\Gamma-\alpha t)) + c_1\cosh(2\sqrt{|\mu\lambda|}(x_1+x_2+\ldots+x_\Gamma-\alpha t)) + c_2}\right].$$

The 2-dimensional plot, 3-dimensional plot and 2-dimensional contour plot of the solution $u_1(t,X)$) have shown in the figure with $\alpha = \frac{1}{3}$, $\beta = \frac{1}{2}$, $\mu = \lambda = 1$,and $c_1 = c_2 = 1$ in intervals $(-20, 20)$ for each plot (Figs. 1–4).

The 2-dimensional plot, 3-dimensional plot and 2-dimensional contour plot of the solution $u_2(t,X)$ have shown in the figure with $\alpha = \frac{1}{3}$, $\beta = \frac{1}{2}$, $\mu = -1$, $\lambda = 1$,and $c_1 = c_2 = 1$ in intervals $(-20, 20)$ for each plot.

The 2-dimensional plot, 3-dimensional plot and 2-dimensional contour plot of the solution $u_3(t,X)$ have shown in the figure with $\alpha = \frac{-1}{3}$, $\beta = \frac{1}{4}$, $\mu = \lambda = 1$,and $c_1 = c_2 = 1$ in intervals $(-20, 20)$ for each plot.

The 2-dimensional plot, 3-dimensional plot and 2-dimensional contour plot of the solution $u_4(t,X)$ have shown in the figure with $\alpha = \frac{1}{3}$, $\beta = \frac{1}{4}$, $\mu = -1$, $\lambda = 1$,and $c_1 = c_2 = 1$ in intervals $(-20, 20)$ for each plot.

Sufficient conditions for the stability of traveling wave solutions

The sufficient conditions for the solitary wave solutions generated are addressed in this section of the paper. The following initiative can be conveyed after doing some investigation.

Proposition

If $u_i(t,X)$, for $i = 1, 2, 3, 4$ is evaluated through the use of the extended$\left(\frac{G'}{G^2}\right)$-expansion method as solitary wave solutions of Eq. (2), then here are all given the sufficient conditions for stability.

Case 1: For the stability of $u_1(t,X)$ here is the sufficient condition:

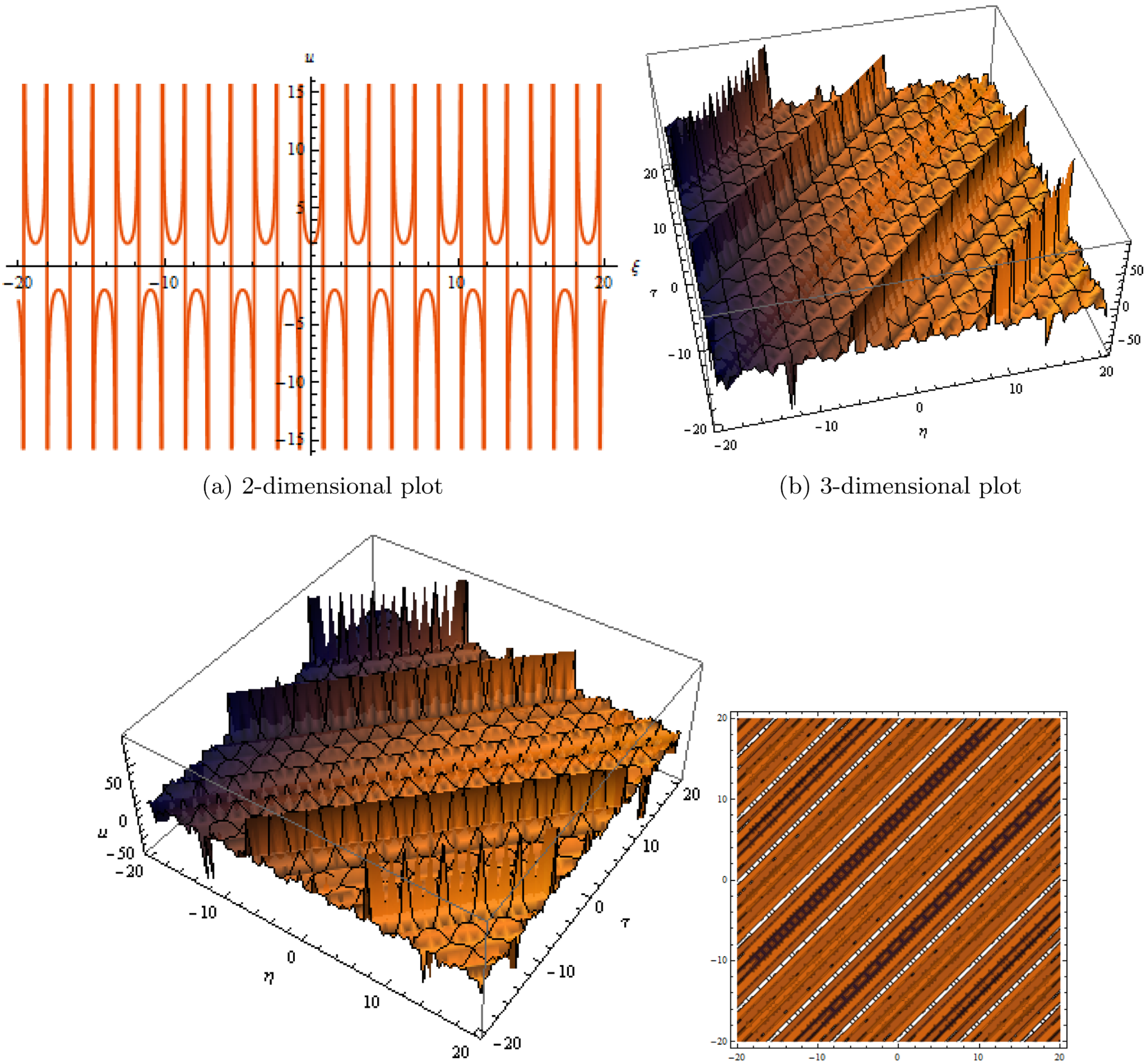

(a) 2-dimensional plot (b) 3-dimensional plot

(c) 3-dimensional (rotated) plot (d) 2-dimensional contour plot

Fig. 1. Set 1 ($\mu\lambda > 0$).

$\left(\frac{3\alpha}{2\beta}\right) > 0$, where $\beta \neq 0$.

Case 2: For the stability of $u_2(t, X)$ here is the sufficient condition:

$\left(\frac{3\alpha}{2\beta}\right) < 0$, where $\beta \neq 0$.

Case 3: For the stability of $u_3(t, X)$ here is the sufficient condition:

$\left(\frac{3\alpha}{\beta}\right) < 0$, where $\beta \neq 0$.

Case 4: For the stability of $u_4(t, X)$ here is the sufficient condition:

$\left(\frac{3\alpha}{\beta}\right) > 0$, where $\beta \neq 0$.

The extended direct algebraic method

Cubic Duffing equation is currently considered here i.e Eq. (51), in this section of the paper, having α, β, and Γ as the real parameters. Our target is to obtain solution for Eq. (51). For travelling wave solutions of Eq. (2), we needs to solve only Eq. (51). After we have balanced highest power of the nonlinear term U^3 along with the highest order derivative term $U_{\xi\xi}$, from Eq. (51), we will achieve $M = 1$, which eventually refers to the pattern called solution:

$$U(\xi) = a_1 + a_2 W(\xi), \tag{55}$$

where $W(\xi)$ satisfies Eq. (11).

After plugging Eq. (55) in Eq. (51), we get a structure of the respective algebraic equations and coefficients of different powers of $W(\xi)$ are equalized.

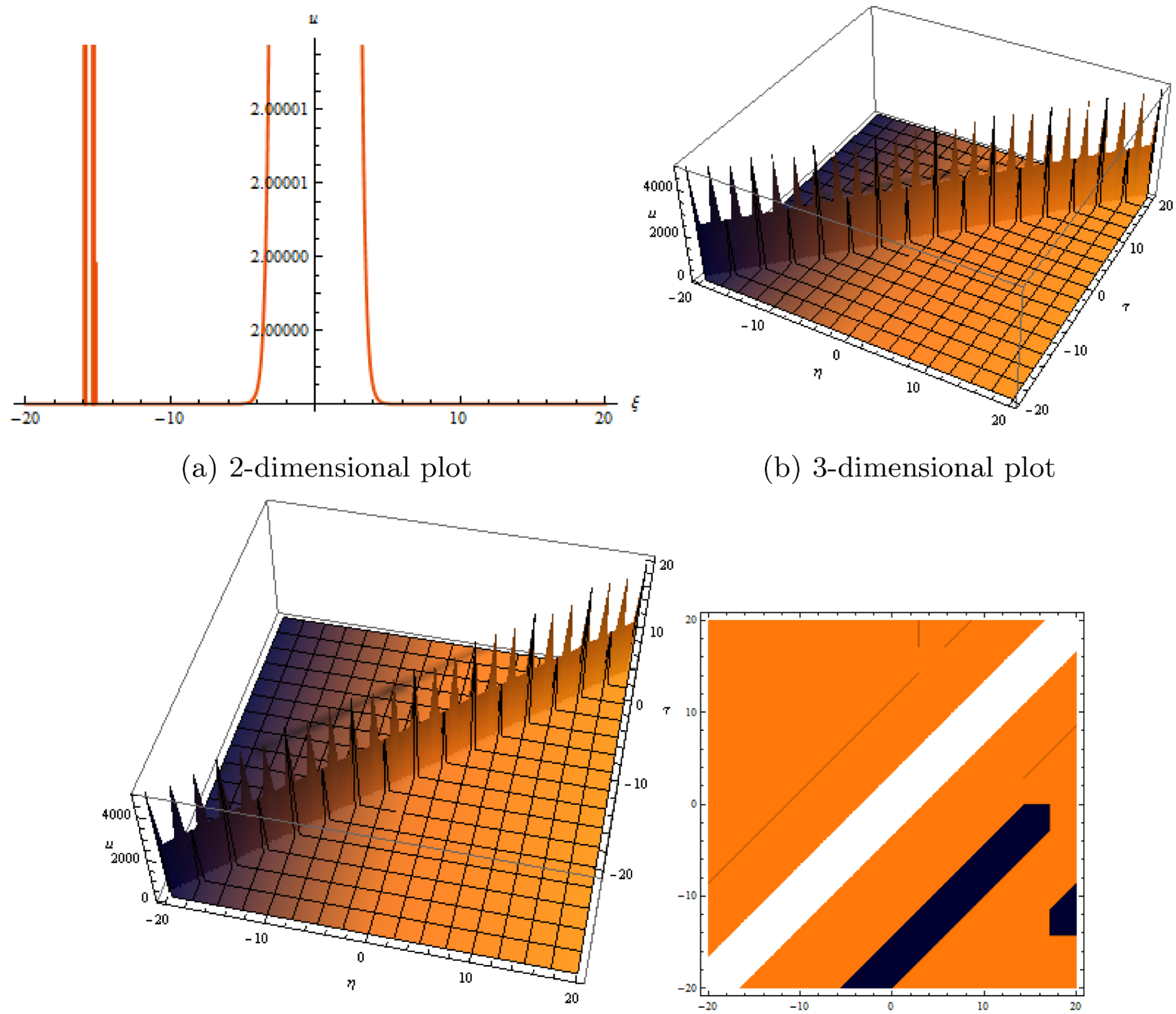

(a) 2-dimensional plot (b) 3-dimensional plot

(c) 3-dimensional (rotated) plot (d) 2-dimensional contour plot

Fig. 2. Set 1 ($\mu\lambda < 0$).

$$W^0(\xi): -\alpha a_1 + \frac{1}{3}\beta a_1^3 + \Gamma\mu\nu a_2\log\rho^2 = 0,$$

$$W^1(\xi): -\alpha a_2 + \beta a_1^2 a_2 + 2\Gamma\zeta\mu a_2\log\rho^2 + \Gamma\nu^2 a_2\log\rho^2 = 0,$$

$$W^2(\xi): \beta a_1 a_2^2 + 3\Gamma\zeta\nu a_2\log\rho^2 = 0,$$

$$W^3(\xi): \frac{1}{3}\beta a_2^3 + 2\Gamma\zeta^2 a_2\log\rho^2 = 0$$

Employing computational program to solve the above algebraic equations, the following set of solution is obtained:

$$a_1 = \pm\nu\sqrt{\frac{3\alpha}{\beta\Phi}}, \quad a_2 = \pm 2\zeta\sqrt{\frac{3\alpha}{\beta\Phi}}, \quad \Gamma = -\frac{2\alpha}{\Phi\log\rho^2}, \tag{56}$$

where

$\Phi = \nu^2 - 4\mu\zeta$.

Set 1. When $\Phi < 0$ along with $\zeta \neq 0$, then.

After plugging the values of a_1 and a_2 via Eq. (56) into Eq. (55) and applying the wave transformation, i.e Eq. (49), which presents the regarding solutions of Eq. (2):

$$u_1(t, X) = \pm\sqrt{\frac{-3\alpha}{\beta}}\left[\tan_\rho\left(\frac{\sqrt{-\Phi}}{2}(x_1 + x_2 + ... + x_m - \alpha t)\right)\right],$$

hence the corresponding solutions are extracted, functioning in much the same line.

$$u_2(t, X) = \pm\sqrt{\frac{-3\alpha}{\beta}}\left[\cot_\rho\left(\frac{\sqrt{-\Phi}}{2}(x_1 + x_2 + ... + x_m - \alpha t)\right)\right],$$

$$\begin{aligned} u_3(t, X) \\ &= \pm\sqrt{\frac{-3\alpha}{\beta}}[\tan_\rho(\sqrt{-\Phi}(x_1) + ... + x_m - \alpha t)) \\ &\pm \sqrt{mn}\sec_\rho(\sqrt{-\Phi}(x_1 + ... + x_m - \alpha t))], \ mn \geqslant 0, \end{aligned}$$

$$\begin{aligned} u_4(t, X) \\ &= \pm\sqrt{\frac{-3\alpha}{\beta}}[\cot_\rho(\sqrt{-\Phi}(x_1 + ... + x_m - \alpha t)) \\ &\pm \sqrt{mn}\csc_\rho(\sqrt{-\Phi}(x_1 + ... + x_m - \alpha t))))], \ mn \geqslant 0, \end{aligned}$$

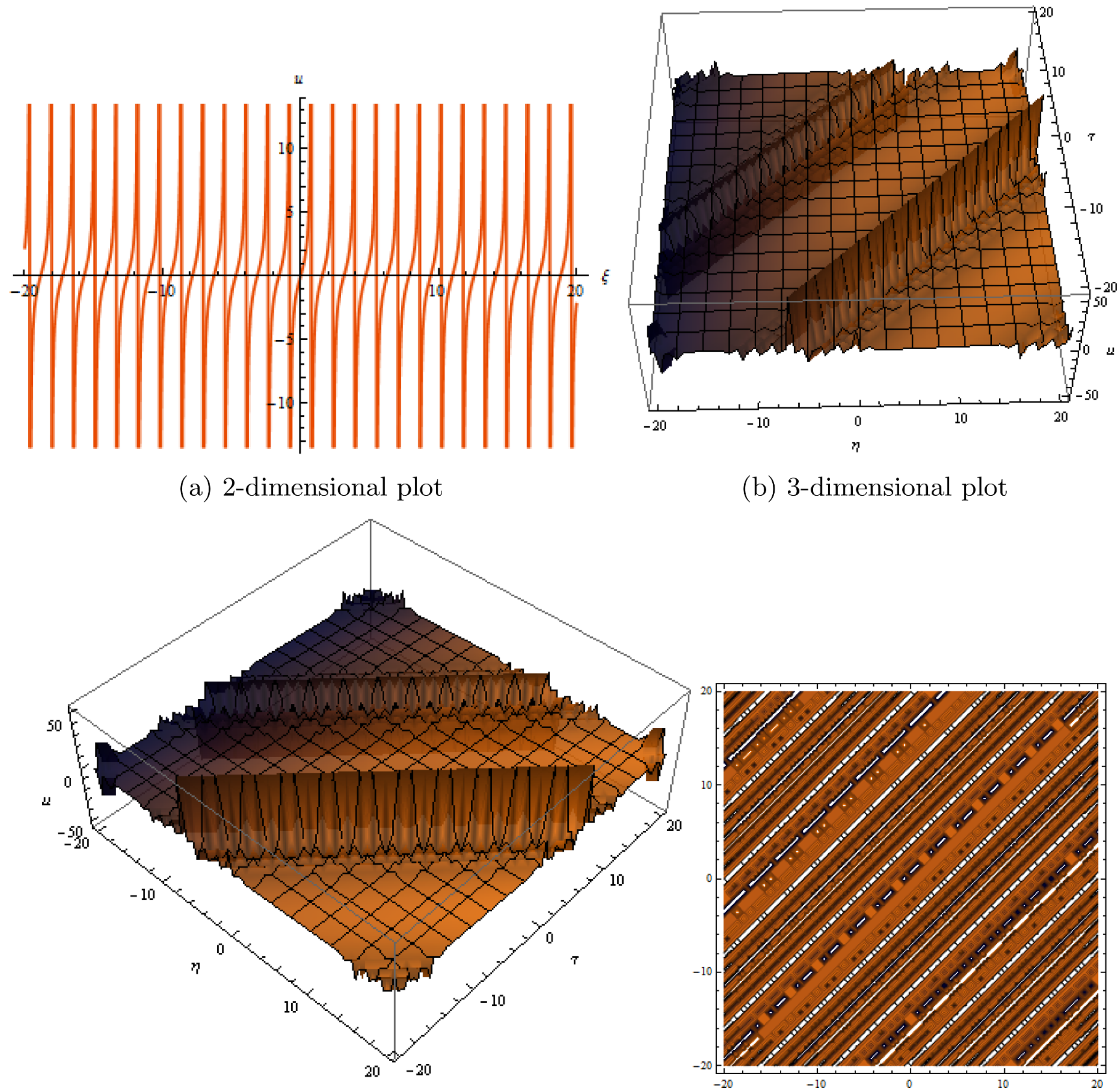

(a) 2-dimensional plot (b) 3-dimensional plot

(c) 3-dimensional (rotated) plot (d) 2-dimensional contour plot

Fig. 3. Set 2 ($\mu\lambda > 0$).

$$u_5(t, X) = \pm\frac{1}{2}\sqrt{\frac{-3\alpha}{\beta}}\left[\tan_\rho\left(\frac{\sqrt{-\Phi}}{4}(x_1+...+x_m-\alpha t)\right)-\cot_\rho\left(\frac{\sqrt{-\Phi}}{4}(x_1+...+x_m-\alpha t)\right)\right].$$

Set 2. When $\Phi > 0$ along with $\zeta \neq 0$, then

$$u_6(t, X) = \pm\sqrt{\frac{3\alpha}{\beta}}\left[\tanh_\rho\left(\frac{\sqrt{\Phi}}{2}(x_1+x_2+...+x_m-\alpha t)\right)\right],$$

$$u_7(t, X) = \pm\sqrt{\frac{3\alpha}{\beta}}\left[\coth_\rho\left(\frac{\sqrt{\Phi}}{2}(x_1+x_2+...+x_m-\alpha t)\right)\right],$$

$$u_8(t, X) = \pm\sqrt{\frac{3\alpha}{\beta}}\,[-\tanh_\rho(\sqrt{\Phi}(x_1+...+x_m-\alpha t)) \pm \sqrt{-mn}\,\mathrm{sech}_\rho(\sqrt{\Phi}(x_1+...+x_m-\alpha t))],\ mn \leqslant 0,$$

$$u_9(t, X) = \pm\sqrt{\frac{3\alpha}{\beta}}\,[-\coth_\rho(\sqrt{\Phi}(x_1+...+x_m-\alpha t)) \pm \sqrt{mn}\,\mathrm{csch}_\rho(\sqrt{\Phi}(x_1+...+x_m-\alpha t))],\ mn \geqslant 0,$$

$$u_{10}(t, X) = \pm\frac{1}{2}\sqrt{\frac{3\alpha}{\beta}}\left[\tanh_\rho\left(\frac{\sqrt{\Phi}}{4}(x_1+x_2+...+x_m-\alpha t)\right)+\coth_\rho\left(\frac{\sqrt{\Phi}}{4}(x_1+x_2+...+x_m-\alpha t)\right)\right].$$

Set 3. When $\mu\zeta > 0$ along with $\nu = 0$, then

$$u_{11}(t, X) = \pm\sqrt{\frac{-3\alpha}{\beta}}\,[\tan_\rho(\sqrt{\mu\zeta}(x_1+x_2+...+x_m-\alpha t))],$$

$$u_{12}(t, X) = \pm\sqrt{\frac{-3\alpha}{\beta}}\,[\cot_\rho(\sqrt{\mu\zeta}(x_1+x_2+...+x_m-\alpha t))],$$

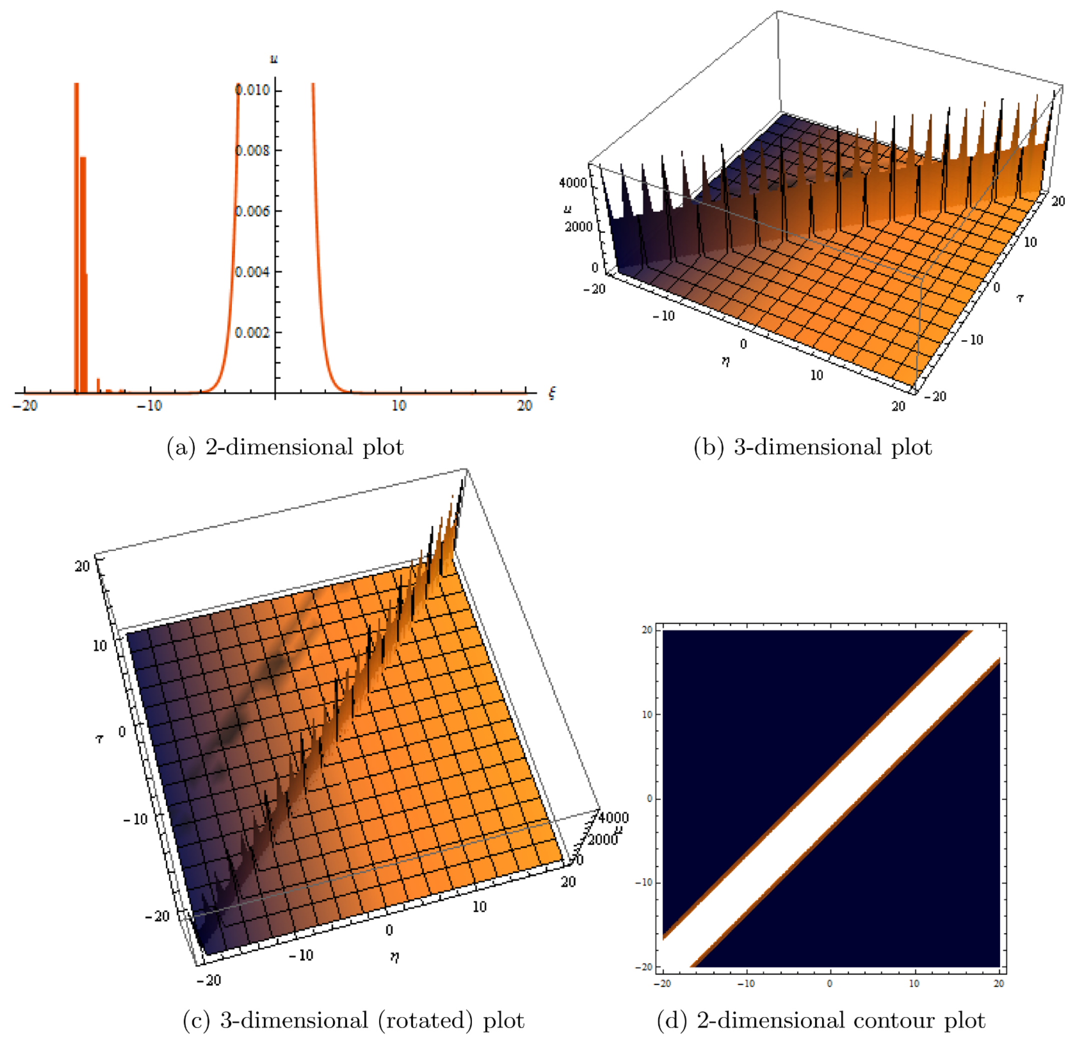

(a) 2-dimensional plot (b) 3-dimensional plot

(c) 3-dimensional (rotated) plot (d) 2-dimensional contour plot

Fig. 4. Set 2 ($\mu\lambda < 0$).

$$u_{13}(t, X) = \pm\sqrt{\frac{-3\alpha}{\beta}}\,[\tan_\rho(2\sqrt{\mu\zeta}(x_1+...+x_m-\alpha t)) \pm \sqrt{mn}\sec_\rho(2\sqrt{\mu\zeta}(x_1+...+x_m-\alpha t))],\ mn \geqslant 0,$$

$$u_{14}(t, X) = \pm\sqrt{\frac{-3\alpha}{\beta}}\,[-\cot_\rho(2\sqrt{\mu\zeta}(x_1+...+x_m-\alpha t)) \pm \sqrt{mn}\csc_\rho(2\sqrt{\mu\zeta}(x_1+...+x_m-\alpha t))],\ mn \geqslant 0,$$

$$u_{15}(t, X) = \pm\frac{1}{2}\sqrt{\frac{-3\alpha}{\beta}}\left[\tan_\rho\left(\frac{\sqrt{\mu\zeta}}{2}(x_1+...+x_m-\alpha t)\right) - \cot_\rho\left(\frac{\sqrt{\mu\zeta}}{2}(x_1+...+x_m-\alpha t)\right)\right].$$

Set 4. When $\mu\zeta < 0$ along with $\nu = 0$, then

$$u_{16}(t, X) = \pm\sqrt{\frac{-3\alpha}{\beta}}\,[\tanh_\rho(\sqrt{-\mu\zeta}(x_1+x_2+...+x_m-\alpha t))],$$

$$u_{17}(t, X) = \pm\sqrt{\frac{-3\alpha}{\beta}}\,[\coth_\rho(\sqrt{-\mu\zeta}(x_1+x_2+...+x_m-\alpha t))],$$

$$u_{18}(t, X) = \pm\sqrt{\frac{-3\alpha}{\beta}}\,[-\tanh_\rho(2\sqrt{-\mu\zeta}(x_1+..+x_m-\alpha t)) \pm \sqrt{-mn}\,\mathrm{sech}_\rho(2\sqrt{-\mu\zeta}(x_1+..+x_m-\alpha t))],\ mn \leqslant 0,$$

$$u_{19}(t, X) = \pm\sqrt{\frac{-3\alpha}{\beta}}\,[-\coth_\rho(2\sqrt{-\mu\zeta}(x_1+x_2+..+x_m-\alpha t)) \pm \sqrt{mn}\,\mathrm{csch}_\rho(2\sqrt{-\mu\zeta}(x_1+x_2+..+x_m-\alpha t))],\ mn \geqslant 0,$$

$$u_{20}(t, X) = \pm\frac{1}{2}\sqrt{\frac{-3\alpha}{\beta}}\left[\tanh_\rho\left(\frac{\sqrt{-\mu\zeta}}{2}(x_1+x_2+..+x_m-\alpha t)\right) + \coth_\rho\left(\frac{\sqrt{-\mu\zeta}}{2}(x_1+x_2+..+x_m-\alpha t)\right)\right].$$

Set 5. When $\nu = 0$ along with $\mu = \zeta$, then

$$u_{21}(t, X) = \pm\sqrt{\frac{-3\alpha}{\beta}}\,[\tan_\rho(\mu(x_1+x_2+..+x_m-\alpha t))],$$

$$u_{22}(t, X) = \pm\sqrt{\frac{-3\alpha}{\beta}}\,[-\cot_\rho(\mu(x_1+x_2+..+x_m-\alpha t))],$$

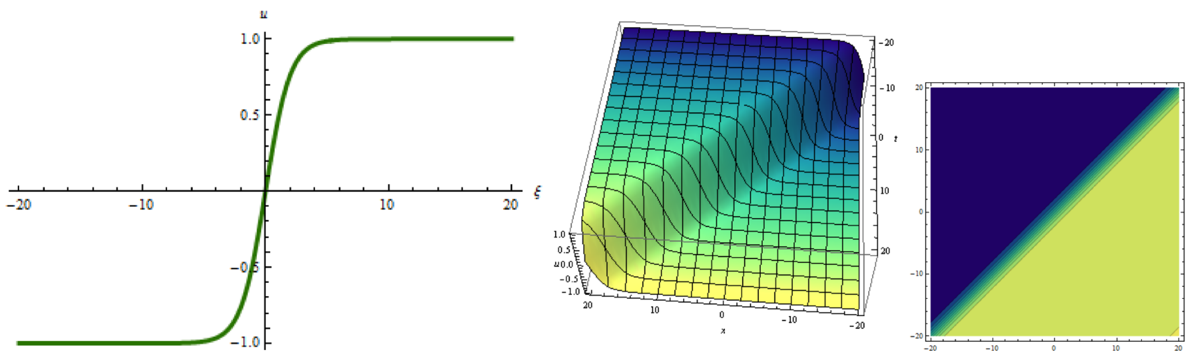

(a) 2-dimensional plot (b) 3-dimensional plot (c) 2-dimensional contour plot

Fig. 5. Set 2 (plot of u_6).

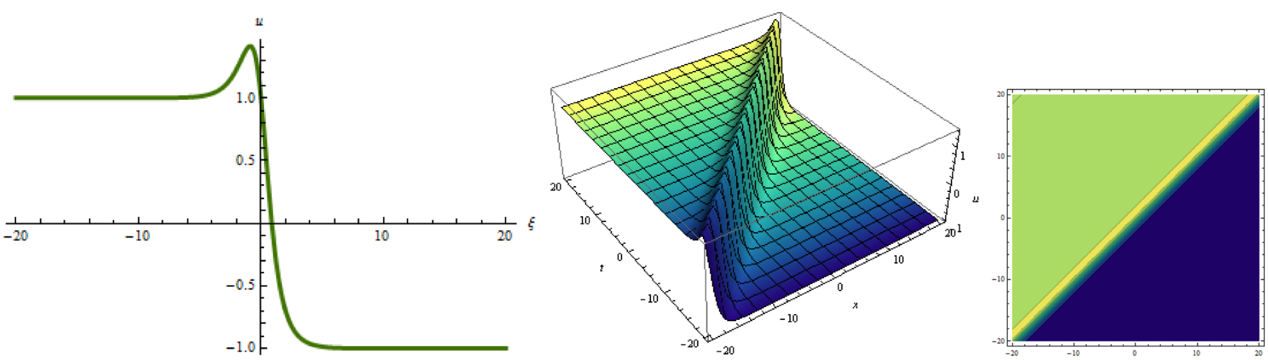

(a) 2-dimensional plot (b) 3-dimensional plot (c) 2-dimensional contour plot

Fig. 6. Set 2 (plot of u_8).

$$u_{23}(t,X) = \pm\sqrt{\frac{-3\alpha}{\beta}}\,[\tan_\rho(2\mu(x_1+x_2+..+x_m-\alpha t)) \pm \sqrt{mn}\,\mathrm{sec}_\rho(2\mu(x_1+x_2+..+x_m-\alpha t))],\ mn \geqslant 0,$$

$$u_{24}(t,X) = \pm\sqrt{\frac{-3\alpha}{\beta}}\,[-\cot_\rho(2\mu(x_1+x_2+..+x_m-\alpha t)) \pm \sqrt{mn}\,\mathrm{csc}_\rho(2\mu(x_1+x_2+..+x_m-\alpha t))],\ mn \geqslant 0,$$

$$u_{25}(t,X) = \pm\frac{1}{2}\sqrt{\frac{-3\alpha}{\beta}}\left[\tan_\rho\left(\frac{\mu}{2}(x_1+x_2+..+x_m-\alpha t)\right) - \cot_\rho\left(\frac{\mu}{2}(x_1+x_2+..+x_m-\alpha t)\right)\right].$$

Set 6. When $\nu = 0$ along with $\zeta = -\mu$, then

$$u_{26}(t,X) = \pm\sqrt{\frac{3\alpha}{\beta}}\,[\tanh_\rho(\mu(x_1+x_2+..+x_m-\alpha t))],$$

$$u_{27}(t,X) = \pm\sqrt{\frac{3\alpha}{\beta}}\,[\coth_\rho(\mu(x_1+x_2+..+x_m-\alpha t))],$$

$$u_{28}(t,X) = \pm\sqrt{\frac{3\alpha}{\beta}}\,[-\tanh_\rho(2\mu(x_1+x_2+..+x_m-\alpha t)) \pm \sqrt{-mn}\,\mathrm{sech}_\rho(2\mu(x_1+x_2+..+x_m-\alpha t))],\ mn \leqslant 0,$$

$$u_{29}(t,X) = \pm\sqrt{\frac{3\alpha}{\beta}}\,[-\cot_\rho(2\mu(x_1+x_2+..+x_m-\alpha t)) \pm \sqrt{mn}\,\mathrm{csch}_\rho(2\mu(x_1+x_2+..+x_m-\alpha t))],\ mn \geqslant 0,$$

$$u_{30}(t,X) = \pm\sqrt{\frac{3\alpha}{\beta}}\left[-\frac{1}{2}\tanh_\rho\left(\frac{\mu}{2}(x_1+x_2+..+x_m-\alpha t)\right) + \cot_\rho\left(\frac{\mu}{2}(x_1+x_2+..+x_m-\alpha t)\right)\right].$$

Set 7. When $\mu = 0$ along with $\nu \neq 0$ then

$$u_{31}(t,X) = \pm\sqrt{\frac{3\alpha}{\beta}}\left[1 - \frac{2m}{(\cosh_\rho(\nu(x_1+x_2+..+x_m-\alpha t)) - \sinh_\rho(\nu(x_1+x_2+..+x_m-\alpha t)) + m)}\right],$$

$$u_{32}(t,X) = \pm\sqrt{\frac{3\alpha}{\beta}}\left[1 - \frac{2(\sinh_\rho(\nu(x_1+x_2+..+x_m-\alpha t)) + \cosh_\rho(\nu(x_1+x_2+..+x_m-\alpha t)))}{\zeta(\sinh_\rho(\nu(x_1+x_2+..+x_m-\alpha t)) + \cosh_\rho(\nu(x_1+x_2+..+x_m-\alpha t)) + n)}\right].$$

Set 8. When $\nu = p$, $\zeta = pq$, ($q \neq 0$ along with $\mu = 0$) then

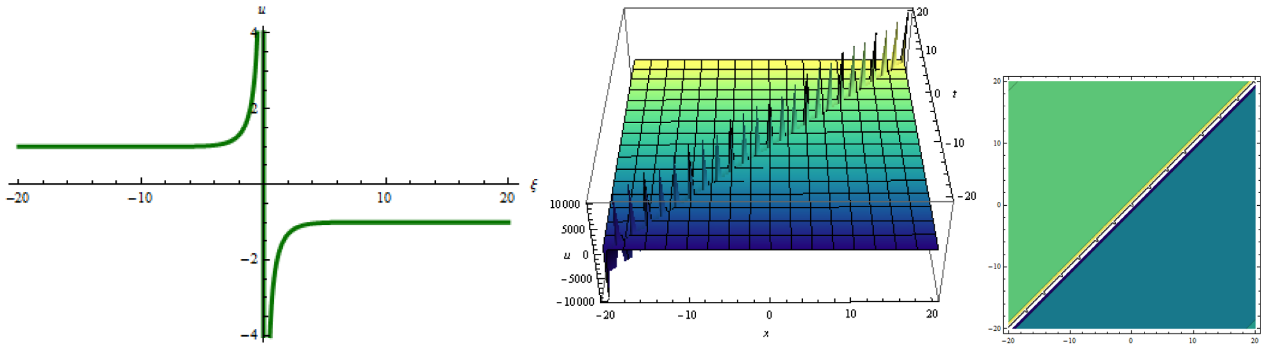

(a) 2-dimensional plot (b) 3-dimensional plot (c) 2-dimensional contour plot

Fig. 7. Set 2 (plot of u_9).

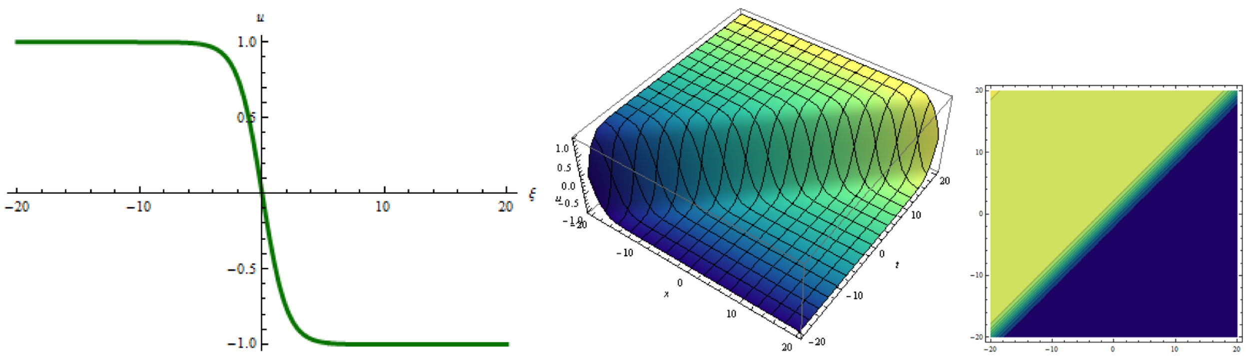

(a) 2-dimensional plot (b) 3-dimensional plot (c) 2-dimensional contour plot

Fig. 8. Set 4 (plot of u_{19}).

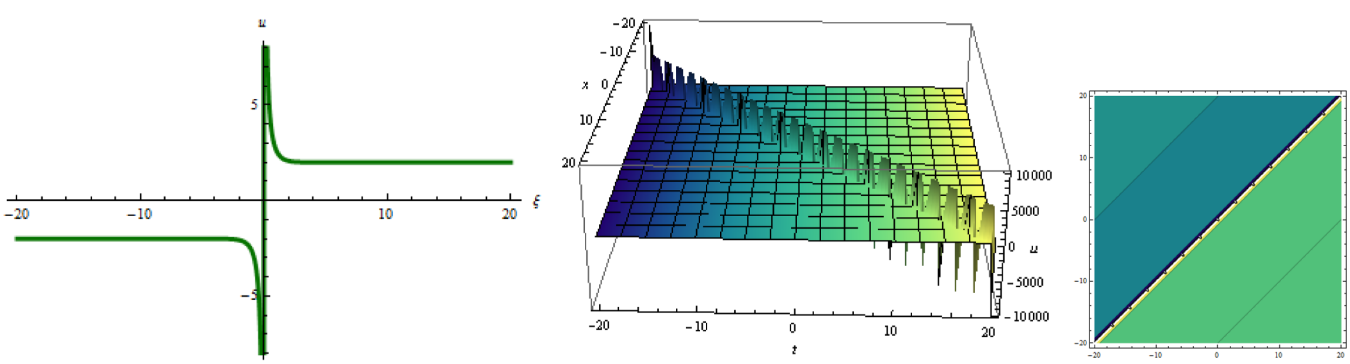

(a) 2-dimensional plot (b) 3-dimensional plot (c) 2-dimensional contour plot

Fig. 9. Set 4 (plot of u_{20}).

$$u_{33}(t, X) = \pm\sqrt{\frac{3\alpha}{\beta}}\left[1 - \frac{2qm\rho^{p(x_1+x_2+..+x_m-\alpha t)}}{m - qn\rho^{p(x_1+x_2+..+x_m-\alpha t)}}\right].$$

Graphical representation of the results

Throughout this portion of the paper, we will describe the graphic portrayal for our whole freshly identified distinguished classes with exact outcomes of the wave transportation, within we have functions combination e.g trigonometric functions, hyperbolic functions, and rational functions. It's essential to acknowledge here that the extraction of these traveling waves belongs to different classes of solitary solutions. Through various relevant latest figures to describe a comprehensive interpretation of the whole graphical representation for modified Zakharov-Kuznetsov equation employing extended direct algebraic method with the help of computational program.

In this section, we will discuss the physical description of set 2 (plots of u_6). The 2-dimensional plot, 3-dimensional plot and 2-dimensional contour plot of the solution $u_6(\xi)$ are presented in the figure respectively. The traveling wave extraction u_6 belongs to family of dark

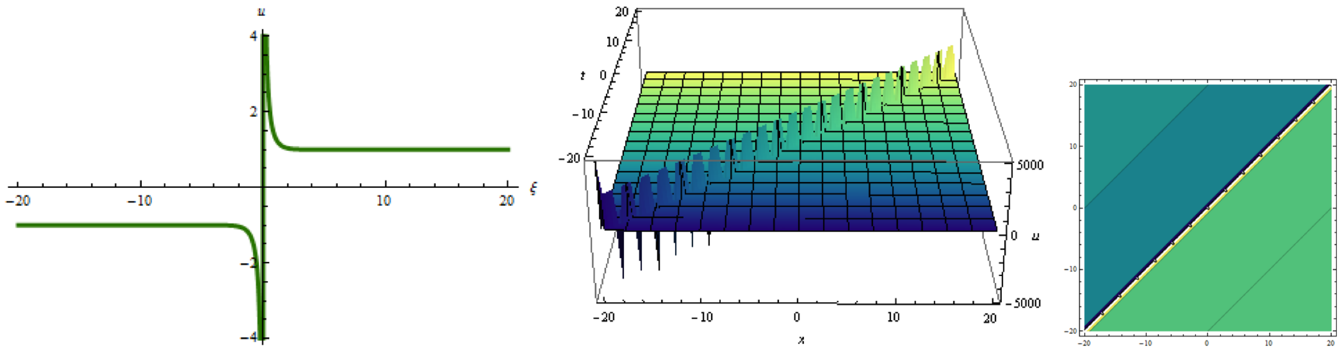

(a) 2-dimensional plot (b) 3-dimensional plot (c) 2-dimensional contour plot

Fig. 10. Set 6 (plot of u_{27}).

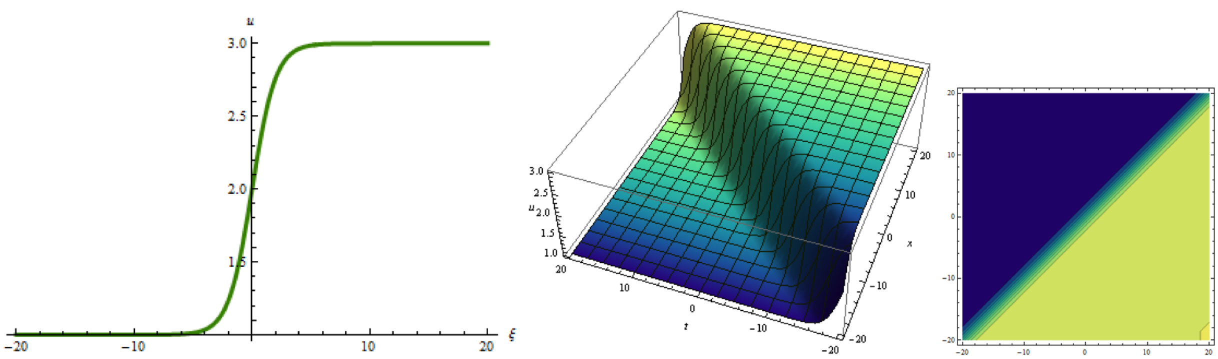

(a) 2-dimensional plot (b) 3-dimensional plot (c) 2-dimensional contour plot

Fig. 11. Set 8 (plot of u_{33}).

solitary solutions. The graphical interpretation of Fig. 5, with $\rho = e$, $\mu = \frac{1}{4}$, $\zeta = 3$, $\nu = 2$, $\alpha = 1$, $\beta = 3$, in intervals $(-20, 20)$ for each plot.

Since the transformation we use is $\xi = x_1 + x_2 + x_3 + \ldots + x_\Gamma - \alpha t$,its important to mention that we use ξ, as variable for 2-dimensional plots and 2-dimensional contour plots also for 3-dimensional plots we use $(x - t)$, as variable. Moreover, it should be noted here that not only u_6, but also u_{16} and u_{26} are the part of the dark community of solitary outcomes.

Here is physical representation of set 2 (plots of u_8). The 2-dimensional plot, 3-dimensional plot and 2-dimensional contour plot of the solution $u_8(\xi)$ are displayed in the figure respectively. Here the taking out traveling wave u_8 belongs to group of semi-bright solitary solutions. The description for graphical interpretation of Fig. 6, with $\rho = e$, $\alpha = 1$, $\beta = 3$, $\mu = \frac{1}{4}$, $\zeta = 3$, $\nu = 2$, $m = -1$ and $n = 1$ in intervals $(-20, 20)$ for each plot. Similarly as in above case there would be realize here in u_8, also with u_{18} and u_{28} are related with the family of semi-bright solitary outcomes.

The physical analysis of set 2 (plots of u_9) is examine here in the section. The 2-dimensional plot, 3-dimensional plot and 2-dimensional contour plot of the solution $u_9(\xi)$ respectively, have shown in the figure. Here solution u_9 belongs to the group of singular solitary solutions along with Type 1 and 2. The description for graphical interpretation of Fig. 7, with $\rho = e$, $\alpha = 1$, $\beta = 3$, $\mu = -\frac{1}{2}$, $\zeta = \frac{1}{2}$, $\nu = 0$, $m = 1$ and $n = 1$ in intervals $(-20, 20)$ for each plot. As already in the above case, there we can see that u_9, also with u_{19} and u_{29} are related with a group of singular solitary solutions along with Type 1 and 2.

Here is physical analysis of set 4 (plots of u_{19}). The 2-dimensional plot, 3-dimensional plot and 2-dimensional contour plot of the solution $u_{19}(\xi)$ respectively, have shown in the figure. Here solution u_{19} belongs to the group of singular solitary solutions along with Type 1 and 2. The description for graphical interpretation of Fig. 8, with $\rho = e$, $\alpha = 1$, $\beta = 3$, $\mu = \frac{-1}{2}$, $\zeta = \frac{1}{2}$, $\nu = 0$, $m = 1$ and $n = 1$ in intervals $(-20, 20)$ for each plot.

Here is physical analysis of set 4 (plots of u_{20}). The 2-dimensional plot, 3-dimensional plot and 2-dimensional contour plot of the solution $u_{20}(\xi)$ respectively, have shown in the figure. Here solution u_{20} belongs to the category of singular-dark solitary solutions. The description for physical interpretation of Fig. 9, with $\rho = e$, $\alpha = 1$, $\beta = \frac{3}{4}$, $\mu = -1$, $\zeta = 1$, and $\nu = 0$, in intervals $(-20, 20)$ for each plot. Hence as already discussed above, we can see here u_{20}, also with u_{10} and u_{30} are related to the class of singular-dark solitary solutions.

Here is physical analysis of set 6 (plots of u_{27}). The 2-dimensional plot, 3-dimensional plot and 2-dimensional contour plot of the solution $u_{27}(\xi)$ respectively, have shown in the figure. Here u_{27} belongs to the group of singular solitary solutions along with Type 2. The description for physical interpretation of Fig. 10, with $\rho = e$, $\alpha = 1$, $\beta = 3$, and $\mu = 1$, in intervals $(-20, 20)$ for each plot. Hence as already discussed above, we can see here u_{27}, also with u_7 and u_{17} are related to the class of singular solitary solution of Type 2.

Here is physical analysis of set 8 (plots of u_{33}). The 2-dimensional plot, 3-dimensional plot and 2-dimensional contour plot of the solution $u_{33}(\xi)$ have shown in the figure. The description for physical interpretation of Fig. 11, with $\rho = e$, $\alpha = 1$, $\beta = 3$, $m = 1$, $n = 1$, $p = 1$,and $q = -1$,in intervals $(-20, 20)$ for each plot.

Concluding remarks

For exact solutions of $(1 + n)$-dimensional mZK equation is discussed yet in this research paper. In either the existence of the constant magnetic field, the problem embodiments of weakly nonlinear raveling waves in or around a plasma containing cold ions and hot isothermal electrons are provided nonlinear $(1 + n)$-dimensional mZK equation. We demonstrate traveling wave solutions yet for the nonlinear $(1 + n)$-dimensional mZK equation first by applying the extended $(\frac{G'}{G^2})$-expansion method along with the extended direct algebraic method. Such methods are credible and efficient in extracting exact solutions of the nonlinear differential equation. The stability evaluation for even the solutions to the traveling wave is addressed with regards to the sufficient conditions. We also saw the different categories of solitary solutions in the two methods discussed in terms of dark, semi-bright, dark singular, singular soliton of Type 1, and 2 also there mention, sufficient conditions for stability and existence of the solutions of the traveling wave are depend upon involved parameters. All such solutions can be important and valuable in plasma physics like magnetized plasma, in which this equation has been modeled and employed for some specific physical patterns. We have been using the fully ready-made computational program package to resolve the actual problem. By utilizing the same software, we showed graphically the physical representation of extracted solutions. Since the extended direct algebraic method is one of the most general methods that covers different types of traveling wave solutions. Hence, the results computed in this paper are more general to [15]. We also carried out a comprehensive analysis between the traveling waves extracted, along with some of the solutions accessible in the literature. A quick and sharp examination declared that several of the soliton solutions identified are more general, new, and maybe valuable and important in physical applications also not yet published in the literature.

CRediT authorship contribution statement

Adil Jhangeer: Investigation, Methodology, Data curation. **Maham Munawar:** Validation, Writing - review & editing. **Muhammad Bilal Riaz:** Software, Validation. **Dumitru Baleanu:** Conceptualization, Supervision, Project administration.

Declaration of Competing Interest

The authors declare that they have no known competing financial interests or personal relationships that could have appeared to influence the work reported in this paper.

References

[1] Bekir A, Boz A. Exact solutions for nonlinear evolution equations using Exp-function method. Phys Lett A 2008;372:1619–25.
[2] Wang ML, Li XZ. Extended F-expansion method and periodic wave solutions for the generalized Zakharov equations. Phys Lett A 2005;343:48–54.
[3] Tian B, Gao YT. Spherical nebulons and Backlund transformation for a space or laboratory unmagnetized dusty plasma with symbolic computation. Eur Phys J D 2005;33:59–65.
[4] Tian L, Yin J. Stability of multi-compacton solutions and Backlund transformation in K(m, n,1). Chaos, Solitons Fractals 2005;23:159–69.
[5] Seadawy AR. Stability analysis solutions for nonlinear three-dimensional modified Korteweg-de Vries-Zakharov-Kuznetsov equation in a magnetized electron-positron plasma. Phys A: Stat Mech Appl Phys A 2016;455:44–51.
[6] Fan E. Extended Tanh-function method and its applications to nonlinear equations. Phys Lett A 2000;277:212–8.
[7] Wazwaz M. The extended tanh method for new compact and noncompact solutions for the KP-BBM and the ZK-BBM equations. Chaos, Solitons Fract 2008;38:1505–16.
[8] Liu GT, Fan TY. New applications of developed jacobi elliptic function expansion methods. Phys Lett A 2005;345:161–6.
[9] Liu S, Fu Z, Liu SD, Zhao Q. Jacobi elliptic function expansion method and periodic wave solutions of nonlinear wave equations. Phys. Lett. A 2001;289:6974.
[10] Wazwaz A. Distinct variants of the KdV equation with compact and noncompact structures. Appl Math Comput 2004;150:365–77.
[11] Wang M, Zhou Y, Li Z. Application of homogeneous balance method to exact solutions of nonlinear equations in mathematical physics. Phys Lett A 1996;216:67–75.
[12] Moussa MHM, El Shikh RM. Two applications of the homogeneous balance method for solving the generalized Hirota-Satsuma coupled KdV system with variable coefficients. Int J Nonlinear Sci 2009;7:29–38.
[13] Wang X, Li J. The $(\frac{G'}{G})$-expansion method and travelling wave solutions of nonlinear evolution equations in mathematical physics. Phys Lett A 2008;372:417–23.
[14] Zakharov VE, Kuznetsov EA. Three-dimensional solitons. Soviet Physics Uspekhi 1974;39:285–6.
[15] Ali MN, Seadawy AR, Husnine SM. Lie point symmetries, conservation laws and exact solutions of (1 + n)-dimensional modified Zakharov-Kuznetsov equation describing the waves in plasma physics. Pramana – J Phys 2018;91:0048.
[16] Baleanu D, lnc M, Yusuf A, Aliyu AI. Lie symmetry analysis, exact solutions and conservation laws for the time fractional modified zakharov-kuznetsov equation. Nonlinear Anal: Modell Control 2017;22:861–76.
[17] Tracinà R. On the nonlinear self-adjointness of the Zakharov-Kuznetsov equation. Commun Nonlinear Sci Numer Simul 2014;19:377–82.
[18] Jiang YL, Lu Y, Chen C. Conservation Laws and optimal system of extended quantum Zakharov-Kuznetsov equation. J of Nonlinear Math Phys 2016;23:157–66.
[19] Naz R, Ali Z, Naeem I. Reductions and new exact solutions of ZK, Gardner KP, and modified KP equations via generalized double reduction theorem. Abstract Appl Anal 2013;340564:11.
[20] Mothibi DM, Khalique CM. Conservation Laws and Exact Solutions of a Generalized Zakharov-Kuznetsov Equation. Symmetry 2015;7:949–61.
[21] Munro S, Parkes EJ. The stability of obliquely-propagating solitary-wave solutions to a modified Zakharov-Kuznetsov equation. J. Plasma Phys 2004;70:543–52.
[22] Munro S, Parkes EJ. The derivation of a modified Zakharov-Kuznetsov equation and the stability of its solutions. J. Plasma Phys 1999;62:305–17.
[23] Pelinovsky DE, Grimshaw RHJ. An asymptotic approach to solitary wave instability and critical collapse in long-wave KdV-type evolution equations. Physica D 1996;98:139–55.
[24] Sipcic R, Benney DJ. Lump interactions and collapse in the modified Zakharov-Kuznetsov equation. Stud Appl Math 2000;105:385–403.
[25] Shi YR, Xu XJ, Wu ZX, Wang YH, Yang HJ, Duan WS, Lv KP. Application of the homotopy analysis method to solving nonlinear evolution equations. Acta Physica Sinica 2006;55:1555–60.
[26] Zhao XS, Zhou HX, Tang YN, Jia HB. Travelling wave solutions for modified Zakharov-Kuznetsov equation. Appl Math Comput 2006;181:634–48.
[27] Wazwaz AM. The extended tanh method for the Zakharov-Kuznetsov (ZK) equation, the modified ZK equation, and its generalized forms. Commun Nonlinear Sci Numer Simul 2008;13:1039–47.
[28] Tascan F, Bekir A, Koparan M. Travelling wave solutions of nonlinear evolution equations by using the first integral method. Commun Nonlinear Sci Numer Simulat 2009;14:1810–5.
[29] Zhen HL, Tian B, Zhong H, Jiang Y. Dynamic behaviors and soliton solutions of the modified Zakharov-Kuznetsov equation in the electrical transmission line. Comput Math Appl 2014;68:579–88.
[30] El-Taibany WF, Mamunc AA, El-Shorbagy KhH. Nonlinear electrostatic perturbations in a degenerate electron-positron plasma. Adv Space Res 2012;50:101–7.
[31] Seadawy AR. Nonlinear wave solutions of the three-dimensional Zakharov-Kuznetsov-Burgers equation in dusty plasma. Physica A 2015;439:124–31.
[32] Biswas A, Zerrad E. Solitary wave solution of the Zakharov-Kuznetsov equation in plasmas with power law nonlinearity. Nonlinear Anal RWA 2010;11:3272.
[33] Seadawy AR. Nonlinear wave solutions of the three-dimensional Zakharov-Kuznetsov-Burgers equation in dusty plasma. Physica A 2015;439:124–31.
[34] Seadawy AR. New exact solutions for the KdV equation with higher order nonlinearity by using the variational method. Comput Math Appl 2011;62:3741–55.
[35] Seadawy AR. Traveling wave solutions of the Boussinesq and generalized fifth-order KdV equations by using the direct algebraic method. Appl Math Sci 2012;6:4081–90.
[36] Seadawy AR, El-Rashidy K. Traveling wave solutions for some coupled nonlinear evolution equations by using the direct algebraic method. Math Comput Modell 2013;57:1371–9.
[37] Seadawy AR. Exact solutions of a two-dimensional nonlinear Shrödinger equation. Appl. Math. Lett 2012;25:687–91.
[38] Yokus A, Detecting overlapping communities by seed community in weighted complex networks [Ph.D. thesis], (2011), Turkey, Firat University.
[39] Li L, Li E, Wang M. The $((\frac{G'}{G}), (\frac{1}{G}))$-expansion method and its application to travelling wave solutions of the Zakharov equations. Appl Math J Chin 2010;25:454–62.
[40] Zayed E, Alurrfi K, The $((\frac{G'}{G}), (\frac{1}{G}))$-expansion method and its applications to find the exact solutions of nonlinear pdes for nanobiosciences, Math Prob Eng, (2014).
[41] Sahoo S, Ray SS. Solitary wave solutions for time fractional third order modified KdV equation using two reliable techniques $(\frac{G'}{G})$-expansion method and improved $(\frac{G'}{G})$-expansion method. Physica A 2016;448:265–82.
[42] Akbar MA, Ali NHM, Zayed EME. A generalized and improved $(\frac{G'}{G})$-expansion method for nonlinear evolution equations. Math Prob Eng 2012;22.
[43] Hayek M. Constructing of exact solutions to the KdV and Burgers equations with power-law nonlinearity by the extended $(\frac{G'}{G})$-expansion method. Appl Math Comput 2010;217:212–21.
[44] Naher H, Abdullah FA. New generalized and improved $(\frac{G'}{G})$-expansion method for nonlinear evolution equations in mathematical physics. J Egypt Math Soc 2014;22:390–5.
[45] Zhu S. The extended $(\frac{G'}{G})$-expansion method and travelling wave solution of nonlinear evolution equation. Math Comput Appl 2010;15:924–9.

[46] Guo S, Zhou Y. The extended $(\frac{G'}{G})$-expansion method and its applications to the Whitham-Broer-Kaup-Like equations and coupled Hirota-Satsuma KdVequations. Appl Math Comput 2010;215:3214–21.

[47] Aljahdaly NH. Some applications of the modified $(\frac{G'}{G^2})$ -expansion method in mathematical physics. Results Phys. 2019;13:102272 .

[48] Akram G, Mahak N. Travelling wave and exact solution for the perturbed nonlinear Shrodinger equation with Kerr law nonlinearity. Eur Phys J Plus 2018;133:212.

[49] Nasir Ali M, Osman MS, Husnine SM. On the analytical solutions of conformable time-fractional extended Zakharov-Kuznetsov equation through $(\frac{G'}{G^2})$ -expansion method and the modified Kudryashov method. SeMA 2019;76:15–25.

[50] Meng Y. Expanded $(\frac{G'}{G^2})$ - Expansion Method to Solve Separated Variables for the (2+1)-Dimensional NNV Equation. Hindawi Adv Math Phys 2018;9248174:6.

[51] Rezazadeh H. New soliton solutions of the complex Ginzburg-Landau equation with Kerr law nonlinearity. Optik-Inter J Light Elect Opt 2018;167:218–27.

[52] Jhangeer A, Seadawy AR, Ali F, Ahmed A. New complex waves of perturbed Shrodinger equation with Kerr law nonlinearity and Kundu-Mukherjee-Naskar equation. Results Phys 2020;16. 102816.

[53] M-Alizamini SM, Rezazadeh H, New extended direct algebraic method for the Tzitzeica type evolution equations arising in nonlinear optics, 8, (2020), 28-53.

[54] Ilhan E, Kıymaz IO. A generalization of truncated M-fractional derivative and applications to fractional differential equations. Appl Math Nonlinear Sci 2020;5(1):171–88.

[55] Al-Ghafri KS, Rezazadeh H. Solitons and other solutions of (3 + 1)-dimensional space-time fractional modified KdV-Zakharov-Kuznetsov equation. Appl Math Nonlinear Sci 2019;4(2):289–304.

[56] Cattani C, Paoluzzi A. Boundary integration over linear polyhedra. Computer Aided Design 1990;22(2):130–5.

[57] Ciancio V, Ciancio A, Farsaci F. On general properties of phenomenological and state coefficients for isotropic viscoanelastic media. Physica B: Condensed Matter 2008;403:3221–7.

[58] Singha J, Kumar D, Hammouch Z, Atangana A. A fractional epidemiological model for computer viruses pertaining to a new fractional derivative. Appl Math Comput 2018;316:504–15.

[59] Liu S, Zhou Q, Biswas A, Liu W. Phase-shift controlling of three solitons in dispersion-decreasing fibers. Nonlinear Dyn 2019;98:395–401.

[60] Luan Z, Yan Q, Zhou Q, Liu W. Nonlinear control of M-typed solitons in dispersion management systems. Optik 2019;179:624–7.

[61] Luan Z, Yan Q, Zhou Q, Liu W. Interactions between M-typed solitons based on nonlinear optimization in dispersion management systems. Optik 2019;182:144–7.

[62] Dai CQ, Liu J, Fan Y, Yu DG. Two-dimensional localized Peregrine solution and breather excited in a variable-coefficient nonlinear Schrödinger equation with partial nonlocality. Nonlinear Dyn 2017;88:1373–83.

[63] Cordero A, Jaiswal JP, Torregrosa JR. Stability analysis of fourth-order iterative method for finding multiple roots of nonlinear equations. Appl Math Nonlinear Sci 2019;4(1):43–56.

[64] Cattani C, Rushchitskii YaYa. Cubically nonlinear elastic waves: wave equations and methods of analysis. Int Appl Mech 2003;39(10):1115–45.

[65] Baskonus HM, Bulut H, Sulaiman TA. New complex hyperbolic structures to the Lonngren-wave equation by using SineGordon expansion method. Appl Math Nonlinear Sci 2019;4(1):129–38.

[66] Cattani C. Haar wavelet-based technique for sharp jumps classification. Math Computer Modell 2004;39(2–3):255–78.

[67] Yang XJ, Gao F, A new technology for solving diffusion and heat equation, Thermal Science, 21(1 Part A), 133–140, (2017).

[68] Ozer O, Ozel C. Some results on special continued fractions expansions in real quadratic number fields. J Math Anal 2016;7(4):98–107.

[69] Eskitasçıoglu EI, Aktas MB, Baskonus HM. New complex and hyperbolic forms for Ablowitz-Kaup-Newell-Segur wave equation with fourth order. Appl Math Nonlinear Sci 2019;4(1):105–12.

[70] Guirao JLG, Baskonus HM, Kumar A. Regarding new wave patterns of the newly extended nonlinear (2+1)-dimensional Boussinesq equation with fourth order. Mathematics 2020;8(3):341.

[71] Gao W, Senel M, Yel G, Baskonus HM, Senel B. New complex wave patterns to the electrical transmission line model arising in network system. Aims Math 2020;5(3):1881–92.

[72] Wang C, Nie Z, Xie W, Gao J, Zhou Q, Liu W. Dark soliton control based on dispersion and nonlinearity for third order nonlinear Schrödinger equation. Optik 2019;184:370–6.

[73] Wang YY, Dai CQ, Xu YQ, Zheng J, Fan Y. Dynamics of nonlocal and localized spatiotemporal solitons for a partially nonlocal nonlinear Schrödinger equation. Nonlinear Dyn 2018;92:1261–9.

[74] Li JT, Zhu Y, Han JZ, Qin W, Dai CQ, Wang SH. Scalar and vector multipole and vortex solitons in the spatially modulated cubic-quintic nonlinear media. Nonlinear Dyn 2018;91:757–65.

[75] Liu X, Liu W, Triki H, Zhou Q, Biswas A. Periodic attenuating oscillation between soliton interactions for higher-order variable coefficient nonlinear Schrödinger equation. Nonlinear Dyn 2019;96:801–9.

[76] Wu GZ, Dai CQ. Nonautonomous soliton solutions of variable-coefficient fractional nonlinear Schrödinger equation. Appl Math Lett 2020;106:106365 .

[77] Yang X, Huo D, Hong X. Periodic transmission and control of optical solitons in optical fibers. Optik 2020;216:164752 .

[78] Fan X, Qu T, Huang S, Chen X, Cao M, Zhou Q, Liu W. Analytic study on the influences of higher-order effects on optical solitons in fiber laser. Optik 2019;186:326–31.

[79] Dai CQ, Wang YY, Fan Y, Yu DG. Reconstruction of stability for Gaussian spatial solitons in quintic-septimal nonlinear materials under PT -symmetric potentials. Nonlinear Dyn 2018;92:1351–8.

[80] Chen SJ, Lin JN, Wang YY. Soliton solutions and their stabilities of three (2 + 1)-dimensional PT -symmetric nonlinear Schrödinger equations with higher-order diffraction and nonlinearities. Optik 2019;194:162753 .

[81] Yang XJ, Baleanu D, Lazarevic MP, Cajic MS. Fractional boundary value problems for integral and differential equations with local fractional operators. Thermal Sci 2015;19(3):959–66.

[82] Guan X, Liu W, Zhou Q, Biswas A. Darboux transformation and analytic solutions for a generalized super-NLS-mKdV equation. Nonlinear Dyn 2019;98:1491–500.

[83] Dai CQ, Fan Y, Zhang N. Re-observation on localized waves constructed by variable separation solutions of (1+1)-dimensional coupled integrable dispersionless equations via the projective Riccati equation method. Appl Math Lett 2019;96:20–6.

[84] Wang BH, Wang YY. Fractional white noise functional soliton solutions of a wick-type stochastic fractional NLSE. Appl Math Lett 2020;110:106583 .